Hindawi Publishing Corporation
Advances in Optical Technologies
Volume 2013, Article ID 738427, 8 pages
http://dx.doi.org/10.1155/2013/738427

Research Article

Photonic Processing for Wideband Cancellation and Spectral Discrimination of RF Signals

David M. Benton

L-3 TRL Technology, Unit 19 Miller Court, Severn Drive, Tewkesbury, Gloucestershire GL20 8DN, UK

Correspondence should be addressed to David M. Benton; david.benton@l-3com.com

Received 9 July 2013; Revised 16 October 2013; Accepted 16 October 2013

Academic Editor: Augusto Beléndez

Photonic signal processing is used to implement common mode signal cancellation across a very wide bandwidth utilising phase modulation of radio frequency (RF) signals onto a narrow linewidth laser carrier. RF spectra were observed using narrowband, tunable optical filtering using a scanning Fabry Perot etalon. Thus functions conventionally performed using digital signal processing techniques in the electronic domain have been replaced by analog techniques in the photonic domain. This technique was able to observe simultaneous cancellation of signals across a bandwidth of 1400 MHz, limited only by the free spectral range of the etalon.

1. Introduction

Photonic signal processing offers a new paradigm for processing high bandwidth signals and opens up possibilities for directly processing signals that are modulated onto an optical carrier. The ability to process and manipulate ultrawideband signals enables high-resolution, reconfigurable processing of potentially the entire RF spectrum of signals. It is this potential that has received a lot of attention over the past few decades [1, 2] and is suitably demonstrated through devices such as wideband adaptive microwave filters enabled through coherence and phase control [3]. Photonic technologies are a natural source for delivering increased bandwidth, but also the low loss of fibre optic transmission systems has seen developments in transmitting Radio over Fibre (RoF) and antenna remoting [4, 5]. As requirements for increased data bandwidth develop and as spectral densities increase, with congestion becoming an issue, the need for ever more powerful digital signal processing (DSP) is a constant driver. This has inevitable consequences for size, weight, and power (SWaP) considerations, especially in RF signal monitoring and characterisation equipment. With the RF signal in photonic form and the inherent bandwidth benefits that ensue, there is a natural opportunity for implementing analog signal processing (ASP) techniques and making the processing an inherent part of the optical link [6].

Signal cancellation is conventionally implemented by engineering a version of the target waveform that is matched in amplitude but 180° out of phase (negative feedback) such that the interference of the target and engineered waveforms result in cancellation. This approach can be performed with analog or digital signals but is likely to be limited in its operational bandwidth by frequency dependent phase shifts. Photonic carriers modulated by RF signals are not limited by these frequency dependent phase shifts in circuitry and hence can operate across a much wider bandwidth. Photonic signal processing (the manipulation of light waves rather than digitised signals) can be used to cancel out common wideband RF signals enabling weaker signals to be identified. Whilst cancellation is common in photonic signal processing it has tended to be targeted at sideband removal [7–10]. Suppression of modulation signals in photonic systems with some specific examples of signal cancellation was shown through inversion in an optical amplifier [11]. Single sideband suppression is a common technique in which the signal is made to interfere with a phase shifted version of itself, helping to remove the power residing in the (unmodulated) carrier component.

There have recently been reports of photonic based RF cancellation systems that claim impressive levels of cancellation [12–15], typically 40 dB for broadband signals and a

very impressive 70 dB for single tones. These systems represent the current state of the art in photonic cancellation but have significant differences from the system discussed in this paper. Applications of this technique have focussed on removal of cosite interference where a close proximity transmitter will pose significant problems for a receiver, particularly relevant where jammers are being used and can overwhelm a receiver, significantly reducing its ability to observe weak signals. However, the pairwise nature of signal generation for cancellation does not specifically require one signal to be the reference to be removed. Where the two signal sources are independent cancellation will seek to reduce signal contributions that are common to both sources. Conversely signal contributions unique to one source only will be unaffected and can emphasise the differences between the two sources, which can help with signal gradiometry and source location. In this paper photonic processing techniques (equivalent to ASP) are implemented to demonstrate the proof of principle that not only the signal cancellation but also spectral analysis across a wide bandwidth is attainable by optical means without significant DSP.

2. Photonic Processing and Optical Cancellation

The cancellation of signals common to two independent signal sources, such as two antennas, can be implemented by modulating the RF signal from each antenna onto an optical phase modulator, each incorporated into one arm of a Mach Zehnder interferometer (MZI) and fed from a common laser. Conventional MZI modulators are widely available but are used for applications such as single sideband suppression where only a single input signal is required and the output is amplitude modulated. Using separate phase modulators in each arm allows independent signals to be combined and independent phase control is available for each signal, prior to coherent combination.

The simplest demonstration is where a phase shift of π is imposed upon one of the modulated laser fields by the application of a bias voltage and a photodiode detector can be used to observe the resulting intensity after the two arms are recombined. This setup is shown schematically in Figure 1 for the simplest case.

An electrooptic modulator subject to a sinusoidally oscillating RF electric field of modulation frequency ω_m gives rise to an output field consisting of a series of sidebands centred around the laser carrier frequency represented by (see e.g., [16])

$$E(t) = E_0 \left\{ \sum_{k=0}^{\infty} J_k(\delta) \cos(\omega + k\omega_m) t + \sum_{k=0}^{\infty} (-1)^k J_k(\delta) \cos(\omega - k\omega_m) t \right\}, \quad (1)$$

where $J_k(\delta)$ represents a kth order Bessel function and δ is a modulator characteristic parameter. In the case above two modulated fields $E_1(t)$ and $E_2(t)$ are produced in each modulator, respectively, and then combined. Where one modulator has a π phase change added to the carrier frequency ω, then all terms at frequency $(\omega + k\omega_m)$ can be cancelled in principle. In this arrangement all frequency components must be measured through conventional sampling and spectral powers determined through the Fourier transform.

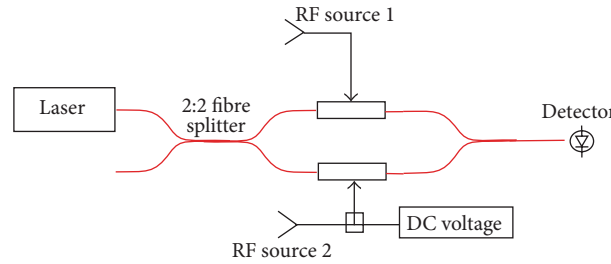

Figure 1: A schematic diagram for observing common mode cancellation in the simplest case.

More generally the RF signals received at each modulator will have a phase difference, due, for example, to time of flight differences from source to antennas. The electric field exiting each modulator can be represented in an ideal set up by

$$E_1(t) = E_0 \cos(\omega t + \delta \sin(\omega_m t + \theta)), \quad (2)$$

$$E_2(t) = E_0 \cos(\omega t + \phi + \delta \sin(\omega_m t)), \quad (3)$$

where θ is the signal phase offset between the received signals, ϕ is the optical phase offset applied to the carrier by the modulator, and each modulator is assumed to receive the same optical amplitude E_0. After application of trigonometric identities and ignoring harmonic terms above $k = 1$ we can write for modulator (1):

$$E_1(t) = E_0 [J_0(\delta) \cos(\omega t) + J_1(\delta) \cos((\omega - \omega_m) t - \theta) - J_1(\delta) \cos((\omega + \omega_m) t + \theta)]. \quad (4)$$

Similarly from modulator (2),

$$E_2(t) = E_0 [J_0(\delta) \cos(\omega t + \phi) + J_1(\delta) \cos((\omega - \omega_m) t + \phi) - J_1(\delta) \cos((\omega + \omega_m) t + \phi)]. \quad (5)$$

The amplitudes from each modulator are combined, with one arm experiencing a π phase shift (due to being a MZI).

In the simple example above involving Nyquist sampling of the detector signal, the amplitude at the modulation frequency will be observed through the mixing within the detector between the modulation signal and the unmodulated carrier. Whilst this provides coherent gain to increase the signal amplitude, it prevents direct comparison of the signal frequencies from each source and is prone to variation as the two carrier components being combined can be cancelled independently from the modulation signals as the carrier phase is varied. It is also possible that a single source of modulation in only one modulator can appear to be cancelled solely through its phase difference with the carrier. To overcome this, the modulation components must be

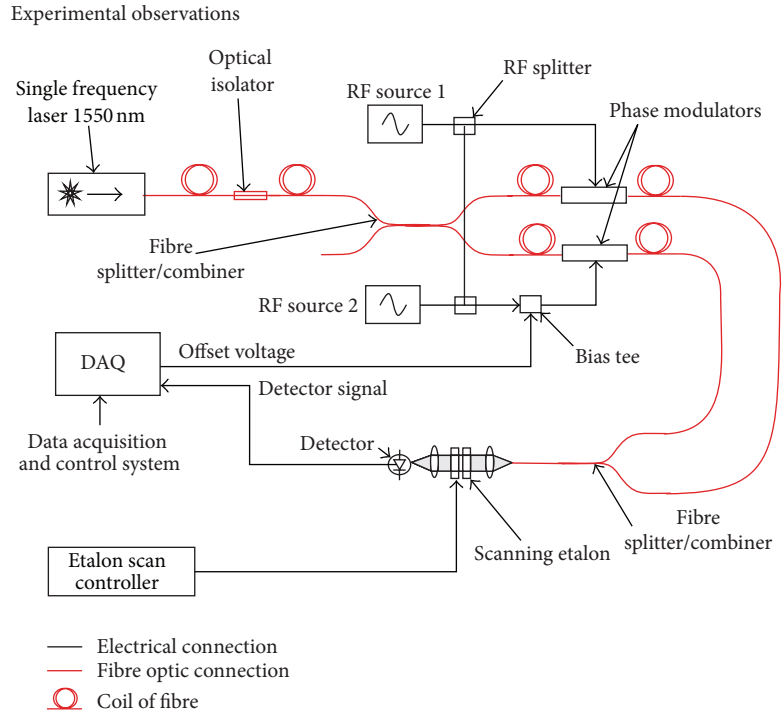

Figure 2: System setup including a scanning Fabry Perot etalon.

separated from the carrier. Separating the carrier frequency from the sidebands can in principle be achieved through dispersion, such as using a diffraction grating. However, a modulation component of 10 MHz has a frequency difference of only 1 part in 10^7 from the unmodulated carrier and would thus require an impractical propagation distance before the modulation component could be spatially separated from the carrier. Separation of the carrier and modulation components is best achieved through filtering. The Fabry Perot etalon (FPE) is in optical terms (though not in RF terms) a high resolution tunable filter, formed of two reflective surfaces (mirrors) accurately separated by a known distance [17]. The transmission through the filter can be tuned by adjusting the spacing between the mirrors and the filter bandwidth which is determined by the level of reflectivity of the mirrors. FPEs with a bandwidth of 10 MHz are commercially available and capable of discriminating between the laser carrier and modulation sidebands. A photodiode detector placed after the FPE measures the intensity being transmitted and the particular mirror separation during a scan determines the frequency to which this intensity relates. Thus the spectral characteristics of the modulation are measured by scanning the FPE filter not by rapid temporal sampling and processing. The spectral bandwidth limitations are those of the FPE and are determined by the free spectral range which can be 10s of GHz. It is also convenient to observe the intensity in both the positive and negative sidebands if required. Thus spectral characteristics across an ultrawide bandwidth can be accessed without recourse to very high speed DSP.

After filtering with the FPE the observed intensity in each sideband arises from the time average of the square of the total amplitude from both modulators. In the positive sideband $\omega+\omega_m$, the observed time averaged intensity is made up of the positive sideband contributions in (4) and (5):

$$\begin{aligned}\left\langle E\left(\omega+\omega_m\right)^2\right\rangle &= \left\langle E_0^2(-J_1\left(\delta\right))^2\right. \\ &\quad\times\left[\cos\left(\left(\omega+\omega_m\right)t+\theta\right)\right. \\ &\quad\left.\left.+\cos\left(\left(\omega+\omega_m\right)t+\phi+\pi\right)\right]^2\right\rangle \\ &= E_0^2 J_1\left(\delta\right)^2\ \left\langle 1-\cos\left(\theta-\phi\right)\right\rangle .\end{aligned} \tag{6}$$

Similarly for the negative sideband $\omega-\omega_m$,

$$\left\langle E\left(\omega-\omega_m\right)^2\right\rangle = E_0^2 J_1\left(\delta\right)^2\ \left\langle 1-\cos\left(\theta+\phi\right)\right\rangle . \tag{7}$$

Thus with a suitable choice of carrier phase offset ϕ, frequency components common to both modulators can be minimised in one or both of the sidebands. Hence the "processing" of cancellation and spectral transform are achieved through only optical means.

3. Experimental Observations

An experimental setup was constructed using commercially available optical fibre based components and is shown in Figure 2. A narrow linewidth laser (100 KHz) operating at 1550 nm with up to 40 mW of power was split into two arms using a 2 : 2 single mode fibre splitter, each of which was connected to a fibre coupled electrooptic phase modulator. The modulated outputs from the phase modulators were recombined with the use of a 2 : 1 splitter/combiner. The output from the recombiner was collimated and then focussed

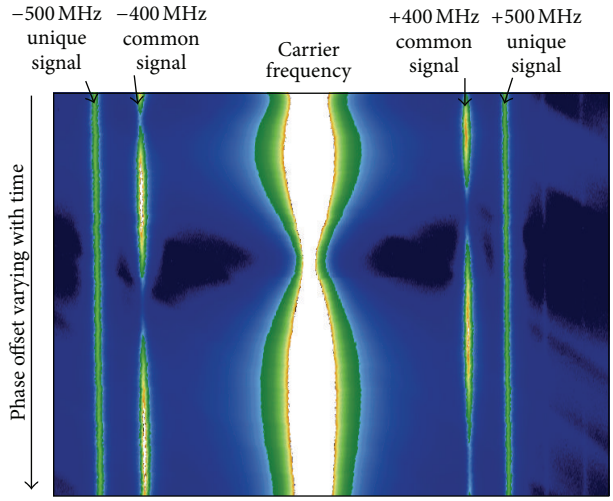

Figure 3: A time evolving spectral plot (waterfall plot) showing positive and negative sidebands around the central carrier frequency. A 400 MHz signal is common to both modulators whilst a 500 MHz signal is present in only one modulator and is unaffected by phase changes.

into a scanning Fabry Perot etalon (FPE). The transmitted output intensity was measured with an amplified photodiode sampled with an ADC within a data acquisition unit (DAQ). Data was collected and processed using a LabView program. RF signals were supplied from a signal generator and directed to each modulator via a splitter. A DC voltage was controlled from the LabView program and applied to one modulator via a bias tee. The LabView program monitored the spectral amplitude at the signal frequency as the DC voltage was systematically varied thereby varying the relative carrier phase between the two arms.

A scanning FPE with a free spectral range of 1.5 GHz and a finesse of 100 was incorporated into the system. This was chosen primarily to give a reasonable compromise between bandwidth (wide in RF terms), resolution (poor in RF terms), and physical size. Whilst significantly higher finesse etalons could be used they are large and cumbersome devices not well suited to use outside of the laboratory. Thus for any system to be widely useful in the real world, size matters. The etalon scan was set to cover a spectral range of 750 MHz either side of the laser carrier frequency so as to prevent confusion with sidebands from the neighbouring free spectral range; thus the effective spectral range is 750 MHz. The scan controller cycled the etalon spacing at a rate of 100 Hz and a detector following the etalon measured the spectral intensity in relation to the filter position. The RF signal amplitude spectral components are related to the optical amplitude seen by the detector. The frequency is determined by the filter position and not by any temporal modulation; thus the spectrum can be obtained with a very low rate sampler, whilst covering a wide spectral range

The detector was sampled at a rate of 10 kSps and related to the scan position using timing gates issued from the etalon scan controller. A time evolving spectral plot (waterfall plot) could be produced to examine the evolution of spectral amplitudes with time and hence with applied voltage (phase). A common signal at 400 MHz (5 dBm) was applied to both modulators via a set of splitters. Another "unique" signal at 500 MHz was applied to just one of the modulators. The plot of Figure 3 shows how the amplitudes of the two signals vary with time as phase changes. In this case a step change was made to the applied voltage and the system was then left to stabilise. The phase varied slowly with time due to thermal effects and the common 400 MHz signal is affected by this in both sidebands. The carrier frequency amplitude is also affected by this phase drift, but the unique 500 MHz signal remains unaffected, thus demonstrating that signal present in only one arm can be discriminated from pervasive common signals.

Some characteristics of this plot need explanation. Firstly the upper and lower sidebands at 400 MHz are out of phase in their response to the phase change. In this case this arises from a difference in the length of the cables connecting the signal generator to the modulators equivalent to a time of flight phase difference in the modulation signal. Secondly the carrier power is cancelled at a different phase to the sidebands. This arises due to a lack of polarisation definition before the laser light enters the modulators. Modulation occurs predominantly for one polarisation state within the modulator and without matching the input polarisation there exist two "modes"—one modulated and one unmodulated—in the output field. The coherent addition of the unmodulated carrier mode and the modulated ($J_0(\delta)$) carrier mode results in a carrier field with an offset phase relative to the sidebands. This situation will be rectified in future with the use of modulators with integral polarisation stages. Nevertheless the proposition that common mode signals can be cancelled is adequately shown here. During the course of these investigations it was observed that the phase applied to the carrier was not linear with applied voltage. This was determined to be due to ohmic heating in the modulator devices, which are impedance matched for use at 10 GHz. The thermal effect upon the refractive index of the modulator material results in a nonlinear phase response, as outlined in the appendix.

To demonstrate that this cancellation can be carried out across a wide instantaneous bandwidth a programmable signal generator was used to repeatedly scan the common modulation frequency in steps of 20 MHz between 100 MHz and 600 MHz, whilst a unique frequency of 500 MHz was maintained in one of the modulators. The offset voltage was then adjusted for maximum suppression of the common signal. In this case the cable length connected to the modulators was matched so that no frequency dependent modulation arising from the RF offset phase was present. The data showing the effect of common signal suppression across a 500 MHz bandwidth is shown in Figure 4 where the cancellation level here is 11 dB across the entire frequency range simultaneously. In this case simultaneous cancellation occurs due to zero relative phase ($\theta = 0$) of the signals at each modulator; thus (6) and (7) are minimised for the same carrier phase.

The amount of cancellation seen here is limited due to a number of contributions. In particular the central carrier frequency is many orders of magnitude more intense than the sidebands and its tail adds noise to the sideband spectral

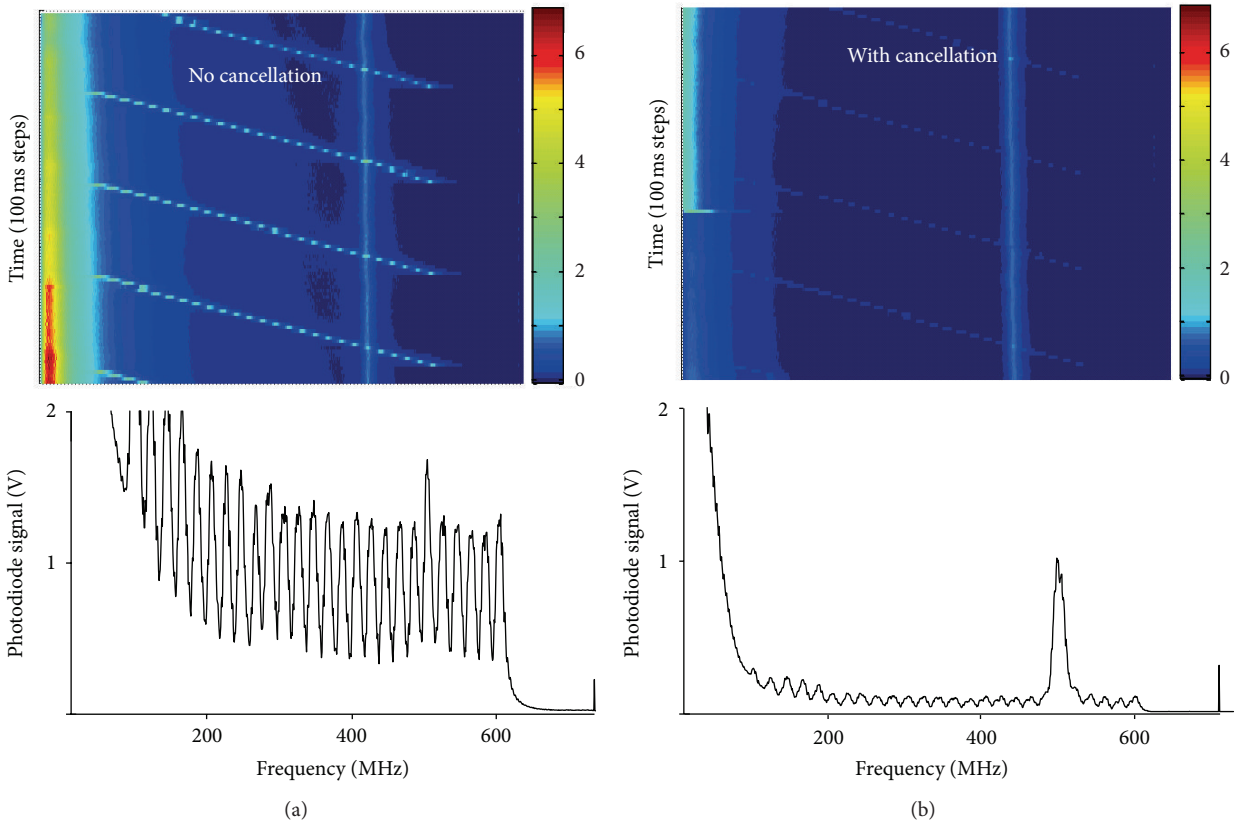

Figure 4: Data plots showing one sideband with a frequency scanning signal in both modulators and unique signal at 500 MHz in only one modulator (a). Simultaneous cancellation of common mode signals across a 500 MHz bandwidth can be seen in the data on (b).

locations. Residual signal can be seen in the suppressed data confirming that cancellation is not complete. The lack of polarisation stage before the modulators leads to differences in the amplitude of the modulated mode which will limit the amount of cancellation that is possible. This can be addressed somewhat by variable attenuators placed after the modulators but this leads to a reduction in overall signal. The isolation offered by the FPE is also imperfect and this adds to the noise level. Modelling has also exposed that the cancellation level is very sensitive to the precise amount of phase offset applied. In this particular case the voltage step resolution corresponded to a phase change of around 0.5° which would limit the cancellation level to 30 dB and hence clearly other contributions were the dominant limitation to the amount of cancellation achieved. Whilst the demonstrated level of cancellation is a little disappointing it is valuable when considering that this system has implemented the dual roles of cancellation and spectral transform without any recourse to high speed sampling or DSP. The cancellation system setup applies equally across a very wide bandwidth, limited here by the free spectral range of the FPE, but in principle can operate across the bandwidth of the modulator. Only an adjustment of modulator offset voltage is required to tune the cancellation for any given frequency and offset signal phase. Cancellation across a range 100–1500 MHz is shown in Figure 5 where higher frequencies are seen entering from right to left and originate from a neighbouring spectral order. There is much potential for improving the performance of this system in subsequent development.

4. Sideband Behaviour

Both upper and lower sidebands can be observed (as seen in Figure 3) and the behaviour of the spectral power in each sideband is dependent upon the relative RF signal phase difference in the two modulators and the carrier phase. The unique signal is however unaffected by the carrier phase and therefore cancellation of common signal can be observed in whatever sideband is most beneficial.

If each modulator is subject to an RF signal obtained via an antenna in a general setting, the distribution of sources in the local environment is likely to be uncontrollable. The received signals will then be subject to a phase difference dependent upon the signal frequency and the spacing of the receiving antennas. Thus cancellation will require a carrier phase setting specific for that source. It can be seen from (6) and (7) that, whatever the phase difference θ of the modulation signal, a value of carrier offset phase can be chosen that will result in cancellation of that modulation signal in either sideband. This can be equivalently seen when a mismatch in cable lengths between signal generator and modulators is introduced, which introduces a frequency dependent phase shift. A cable of length 1 m was introduced before one

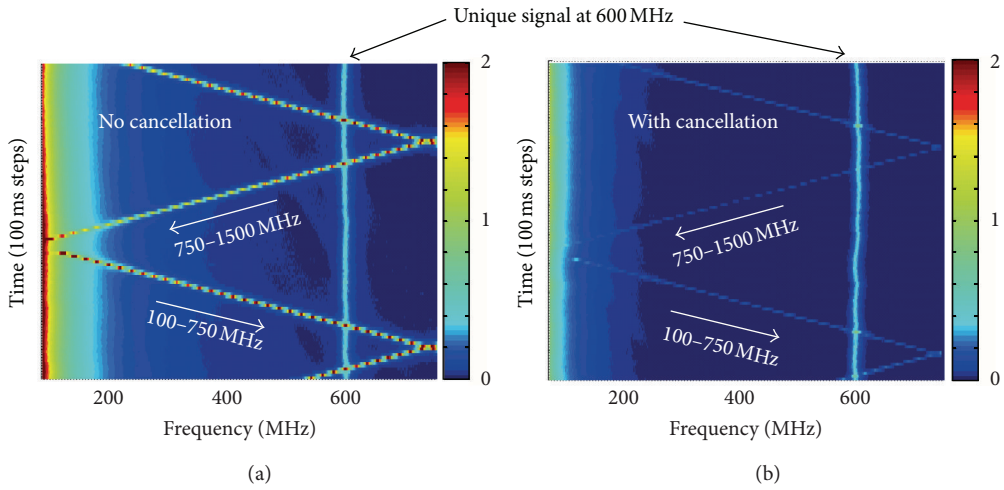

Figure 5: A wideband frequency scanning signal into both modulators with a unique frequency at 500 MHz. Time increases down the diagram and frequencies 100–750 MHz proceed left to right, whilst 750–1500 MHz from neighbouring spectral order proceed right to left. Cancellation is demonstrated in (b).

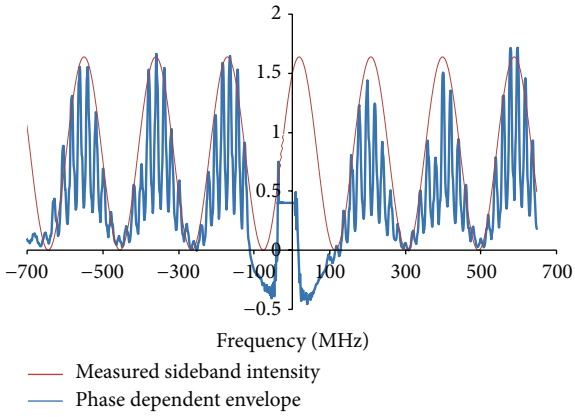

Figure 6: Frequency dependent sideband intensity variations in upper and lower sidebands for a fixed path length difference enroute to the modulators.

modulator. The frequency dependent phase difference $\theta(f)$ is then

$$\theta(f) = \frac{d\varepsilon_r |f|}{c}, \tag{8}$$

where d is the path difference and ε_r is the relative permittivity of the cable. Data was captured encompassing both sidebands where a sequentially varying frequency input was presented to the modulators. The strong, saturated central carrier component was removed from the data by fitting a Lorentzian lineshape (with a half-width of 1.9 MHz and amplitude of 7592). Frequency calibration was carried out with a linear fit to each sideband independently. The envelope of the sideband data was then modelled using the expected frequency dependent phase and is shown in Figure 6. In this case the modelling revealed that the carrier offset phase was set to 60°, which could not be determined independently due to the thermal effects upon the modulators.

5. Improvements and Extensions

Subsequent developments have shown that sharing the offset voltage across both modulators in a push-pull configuration improves stability significantly for two reasons. Firstly whilst the electrooptic phase change is parity dependent, the thermal phase change is not; hence the thermal effects in both modulators have a similar size and the differential effect upon the output phase from the pair of modulators is much reduced. Also because the magnitude of the applied voltage to each modulator is half the required voltage, the power dissipated in each modulator is reduced by a relative factor of 4. A relative test applying a 2 V offset change (from 0 V) was applied comparing application to a single modulator with application across the pair. This has seen the thermal phase drift reduced from 4°/s when applied to a single modulator to 0.8°/s in a push pull-configuration, with the settling time reduced from 200 s to 50 s.

In this paper the intended application has been the comparison of signals from two separate antennas, with the capability of removing signals common to both. In other photonic cancellation work [12, 13] the usage has been predominantly removing a known transmission signal which can be easily obtained and used to provide the feedback reference signal. Using 2 signals from spatially separated antenna would clearly introduce a signal dependent phase offset which is related to the source location relative to the antenna and is the source of the θ term in (6) and (7). Therefore to observe cancellation effects for any particular signal, the carrier phase offset must be adjusted and it is straightforward to conceive of capturing spectra whilst scanning the carrier phase. Indeed given the uncontrollable nature of source locations in the real world, it is necessary to make measurements with at least 2 phase values in order to observe changes in the amount of cancellation taking place. These two measurements should differ by 180° to allow the possibility of maximum and minimum cancellation to

be observed. Knowing the source frequency, the separation of the receiving antennas and relative phase obtained from comparing the sideband strengths allows two possibilities for the angle of arrival to be determined and a measure of source location to be performed. Unambiguous source direction finding would require 3 receivers. Preliminary attempts have shown an angle-of-arrival influence upon the sideband strengths but this requires more investigation and development.

6. Conclusion

This work has demonstrated the basic principle that photonic (analog) processing can be used to implement wideband signal cancellation between two signal sources modulated onto coherent laser carriers using phase modulation. Further to this photonic processing can additionally be used to implement frequency spectrum generation across an ultrawide bandwidth without recourse to high speed sampling, thus replacing the digital signal processing required to perform a Fourier transform. In the case given here filtering is used to separate the sidebands from the carrier in order that unambiguous cancellation effects can be observed, but this is due in part to an inadequacy of the phase modulators used here. In principle significant carrier cancellation can also take place which will help in reducing noise in the final filtered output by reducing the height of the Lorentzian tail of the residual carrier. These are improvements that can be incorporated in future developments, all of which should help to increase the level of cancellation observed at the output detector. The system is suitable for incorporation onto an integrated waveguide system which would significantly reduce the system size and complexity. The current limitation to the system performance is the Fabry Perot etalon where the finesse of 100 limits the isolation between carrier power and sidebands, and the FSR is a limit to the unambiguous bandwidth that can be observed. Etalons with higher finesse and FSR are available but are large, bulky, and cumbersome and hence not well suited to usage outside of laboratory conditions. There are clearly a number of developments that, when implemented, could lead to significant improvements in performance and would form part of a development programme. Nevertheless this is step towards analog signal processing for spectral analysis.

This proof of concept has shown that it is feasible to consider the general case of common mode cancellation of signals across a very wide bandwidth, rather than just the specific case of a cancellation of a single known signal. All that is required is the control of a single voltage level applied to a phase modulator enabling phase scanning and the subsequent observation of the spectrum will reveal the relative phases of common signal components. Further to this there is significance in the observation that signals that are not common to both receivers are unaffected by the cancellation process. This, coupled with observations of the sideband intensities on the positive and negative sides, can reveal information about the spatial distribution of common sources. Converting RF signals into the photonic domain can therefore offer attractive benefits in terms of reducing DSP requirements and acquiring signal source information.

Appendix

The phase offset $\Delta\phi$ from an electrooptic modulator has 2 contributions, the electrooptic effect $\Delta\phi_{\mathrm{EO}}$ and a thermal effect $\Delta\phi_T$:

$$\Delta\phi = \Delta\phi_{\mathrm{EO}} + \Delta\phi_T = \frac{2\pi f L}{c}\left(\Delta n_{\mathrm{EO}} + \Delta n_T\right), \tag{A.1}$$

where Δn is a change in refractive index, f is the applied frequency, L is the length of the modulator, and c is the speed of light.

The electrooptic effect gives a refractive index change:

$$\Delta n_{\mathrm{EO}} = \frac{n_0^3 r\, V \cdot L}{2d}, \tag{A.2}$$

where r is the electrooptic tensor value for the material, V is the applied voltage, d is the electrode gap, and L is the length of the crystal.

The change in temperature ΔT of the device is related to the amount of energy Q deposited through the well-known relation:

$$Q = mC\Delta T, \tag{A.3}$$

where m is the mass of the device and C is the specific heat capacity.

The energy deposited is proportional to the square of the applied voltage $Q \propto (V^2/R)$ leading to

$$\Delta n_T = \frac{dn}{dT}\Delta T = \frac{dn}{dt}\kappa\frac{V^2}{mCR}, \tag{A.4}$$

where κ is a constant.

Thus the phase change has the form

$$\Delta\phi = \frac{2\pi f L}{c}\left(\frac{n_0^3 r_{33}\, V \cdot L}{2d} + \frac{dn}{dt}\,\kappa\frac{V^2}{mCR}\right). \tag{A.5}$$

For $LiNbO_3$ $r_{33} = 30$ pm/V, $dn/dT = 37 \times 10^{-6}/^{\circ}$C.

This form will have the effect of reducing the spacing between consecutive voltages providing a π phase offset. The precise device characteristics are not known and so accurate modelling cannot be performed. However, estimating the electrode gap to be of order 10 μm, the EO component is of the order $n_0^3 \times 10^{-7}$ which is similar in scale to dn/dT. This broadly agrees with the voltage squared dependence observed, but the net result is that thermal effects cause slowly varying phase instability until thermal equilibrium is reached.

References

[1] A. J. Seeds, "Microwave photonics," *IEEE Transactions on Microwave Theory and Techniques*, vol. 50, no. 3, pp. 877–887, 2002.

[2] R. A. Minasian, "Photonic signal processing of microwave signals," *IEEE Transactions on Microwave Theory and Techniques*, vol. 54, no. 2, pp. 832–846, 2006.

[3] F. Zeng and J. Yao, "Investigation of phase-modulator-based all-optical bandpass microwave filter," *Journal of Lightwave Technology*, vol. 23, no. 4, pp. 1721–1728, 2005.

[4] E. I. Ackerman and A. S. Daryoush, "Broad-band external modulation fiber-optic links for antenna-remoting applications," *IEEE Transactions on Microwave Theory and Techniques*, vol. 45, no. 8, pp. 1436–1442, 1997.

[5] D. Novak, T. Clark, S. O'Connor, D. Oursler, and R. Waterhouse, "High performance, compact RF photonic transmitter with feedforward linearization," in *Proceedings of the IEEE Military Communications Conference (MILCOM '10)*, pp. 880–884, October-November 2010.

[6] T. K. Woodward, T. C. Banwell, A. Agarwal, P. Toliver, and R. Menendez, "Signal processing in analog optical links," in *Proceedings of the IEEE Avionics, Fiber-Optics and Photonics Technology Conference (AVFOP '09)*, pp. 17–18, September 2009.

[7] M. Y. Frankel and R. D. Esman, "Optical single-sideband suppressed-carrier modulator for wide-band signal processing," *Journal of Lightwave Technology*, vol. 16, no. 5, pp. 859–863, 1998.

[8] A. Loayssa, J. M. Salvide, D. Benito, and M. J. Garde, "Novel optical single-sideband suppressed-carrier modulator using a bidirectionally-driven electro-optic modulator," in *Proceedings of the International Topical Meeting on Microwave Photonics (MWP '00)*, 2000.

[9] A. Loayssa, J. M. Salvide, D. Benito, and M. J. Garde, "Novel optical single-sideband suppressed-carrier modulator using a bidirectionally-driven electro-optic modulator," in *Proceedings of the International Topical Meeting on Microwave Photonics (MWP '00)*, pp. 117–120, 2000.

[10] A. Siahmakoun, S. Granieri, and K. Johnson, "Double and single side-band suppressed-carrier optical modulator implemented at 1320 nm using LiNbO3 crystals and bulk optics," in *Optoelectric and Wireless Data Management, Processing, Storage, and Retrieval*, vol. 4534 of *Proceedings of SPIE*, pp. 86–92, August 2001.

[11] F. Coppinger, S. Yegnanarayanan, P. D. Trinh, and B. Jalali, "All-optical rf filter using amplitude inversion in a semiconductor optical amplifier," *IEEE Transactions on Microwave Theory and Techniques*, vol. 45, no. 8, pp. 1473–1477, 1997.

[12] M. Alemohammad, D. Novak, and R. Waterhouse, "Photonic signal cancellation for co-site interference mitigation," in *Proceedings of the IEEE Military Communications Conference (MILCOM '11)*, pp. 2142–2146, November 2011.

[13] M. Lu, J. Bruno, Y. Deng, P. R. Prucnal, and A. Hofmaier, "Co-site interference mitigation using optical signal processing," in *Enabling Photonics Technologies for Defense, Security, and Aerospace Applications VIII*, vol. 8397 of *Proceedings of SPIE*, June 2012.

[14] J. Suarez, K. Kravtsov, and P. R. Prucnal, "Incoherent method of optical interference cancellation for radio-frequency communications," *IEEE Journal of Quantum Electronics*, vol. 45, no. 4, pp. 402–408, 2009.

[15] J. Suarez and P. R. Prucnal, "System-level performance and characterization of counter-phase optical interference cancellation," *Journal of Lightwave Technology*, vol. 28, no. 12, pp. 1821–1831, 2010.

[16] A. Yariv, *Optical Electronics*, chapter 9, HRW international, 3rd edition, 1985.

[17] E. Hecht, *Optics*, chapter 9, Addison-Wesley, Reading, Mass, USA, 1987.